

Influence of strain in Ag on Al(111) and Al on Ag(100) thin film growthV. Fournée,^{1,*†} J. Ledieu,² T. Cai,^{1,‡} and P. A. Thiel¹¹Ames Laboratory and Department of Chemistry, Iowa State University, Ames, Iowa 50011²Surface Science Research Centre, The University of Liverpool, Liverpool L69 3BX, United Kingdom

(Received 13 October 2002; revised manuscript received 9 January 2003; published 1 April 2003)

We demonstrate the influence of interfacial strain on the growth modes of Ag films on Al(111), despite the small magnitude of the lattice misfit in this system. The strain is relieved by the formation of stacking fault domains bounded by Shockley partial dislocations. The growth mode and the step roughness appear to be strongly connected. Growth is three-dimensional (3D) as long as the steps are straight, but switches to 2D at higher coverage when the steps become rough. Anisotropic strain relaxation and straight steps seem to be related. We also report related observations for Al deposited on Ag(100).

DOI: 10.1103/PhysRevB.67.155401

PACS number(s): 68.35.Gy, 68.55.-a, 68.37.Ef, 68.47.De

INTRODUCTION

There is currently a broad interest in heteroepitaxial growth, motivated by technological applications such as magnetic data storage and nanoelectronics. Fabrication of these devices requires control of the growth modes adopted by thin films deposited on a substrate material, which can involve rather complex physical mechanisms.

In a well-known series of papers, Bauer established the rules that should prevail in determining the structures of thin films in local thermodynamic equilibrium.^{1,2} In this framework, the balance between the substrate and adsorbate surface energies (γ_s and γ_a , respectively) and the interfacial energy (γ^*) dictates whether the film will grow in a smooth layer-by-layer fashion (if $\gamma_a + \gamma^* \leq \gamma_s$) or three dimensionally (if $\gamma_a + \gamma^* > \gamma_s$). Therefore, layer-by-layer growth is favored if the adsorbate has a low surface energy, but the interfacial energy term needs also to be considered in heteroepitaxy. One component of the interfacial energy is due to the strain that builds up in a heteroepitaxial film, as the result of lattice mismatch. When this component of γ^* increases as growth proceeds, it can switch the free energy balance from a smooth two-dimensional (2D) (layer-by-layer) to 3D (rough) growth at some critical coverage. This intermediate situation is called Stranski-Krastanov growth.

This description, although providing a valuable general guide at a macroscopic level, appears too simplistic relative to the variety of phenomena which have been observed in recent years, in particular with scanning probe microscopies.³ For example, atomic scale observations of the nucleation and growth in several heteroepitaxial systems revealed adsorbate induced surface reconstruction, formation of misfit dislocation networks and/or surface alloying, all related to surface stress relaxation.

Furthermore, the above description in terms of surface and interface free energies assumes that thermodynamic equilibrium prevails during growth. However, this is rarely true because the density of adsorbate atoms during physical vapor deposition usually far exceeds the adsorbate's 2D vapor pressure. Most growth, therefore, occurs out of equilibrium. The film has no time to relax, and its morphology can be strongly affected by kinetic limitations. It is then necessary to obtain a detailed knowledge of the mechanisms and

associated energies of each elementary atomic process involved in film formation, in order to understand and predict the resulting film morphologies.

In this article, we will describe the growth modes observed by scanning tunneling microscopy (STM) in *a priori* simple metal-on-metal epitaxial systems, Ag on Al(111) and Al on Ag(100). Bulk Ag and Al share a common fcc structure, and the lattice mismatch is less than 1%. Therefore, the films should be under negligible stress for both substrates. The surface energies calculated for the (111) and (100) faces of Ag and Al span a range of only 1.17 to 1.34 J/m² and calculated values agree with experimental ones (when available) to within 0.05 J/m².⁴ It seems therefore difficult to predict the growth mode on the basis of the balance between the energy terms. One must rely on experiments.

The growth of Ag films on the Al(111) surface has already been investigated by several techniques including low energy electron diffraction (LEED), Auger electron spectroscopy (AES), X-ray photoemission spectroscopy (XPS), and low-energy ion-scattering spectroscopy (LEIS) (but not with a microscopy). The previous experiments led to contradictory conclusions. Based on LEIS measurements, Losch *et al.*⁵ reported pseudomorphic growth, at least for Ag coverages up to 2 ML at room temperature, with a layer sequence in agreement with fcc stacking. On the other hand, Kim *et al.*⁶ reported the disappearance of the LEED pattern for coverages between 2 and 4 ML at room temperature. After 4 ML, the LEED pattern started to reappear. The proposed explanation involved the formation of an interfacial alloy (hexagonal δ -Ag₂Al) with hcp stacking in parts of the surface, the remaining being covered by Ag islands with fcc stacking. This is surprising, as Ag and Al have almost no miscibility at room temperature. When Kim *et al.*⁶ repeated the LEED experiment at 50 K, the loss of long range order was less dramatic than at room temperature. This led the authors to suggest that formation of the interfacial alloy is inhibited by reduced interdiffusion of Al and Ag at sufficiently low temperature. The idea of surface alloying was supported by x-ray photoemission spectra (XPS) indicating a shift of the Ag 3d_{5/2} binding energy (BE) in this coverage regime, consistent with the BE shift measured for bulk Ag₂Al. It was also suggested that layer-by-layer growth occurs for coverages larger than 5 ML based on LEED *I/V* analysis. This is in

contrast to Ag on Ag(111) homoepitaxy, where limited interlayer transport caused by the step edge barrier results in 3D growth.^{7,8} It was proposed that the large density of kink sites originating from the boundaries of stacking-fault islands could offer channels with reduced step edge barriers to promote interlayer diffusion.

The growth of Al films on Ag(110) and Ag(111) surfaces has also been investigated by LEED, AES, and photoemission spectroscopies,⁹ but not on Ag(100). The authors of those studies concluded that an intermetallic compound, most likely δ -Ag₂Al, is formed at the interface for submonolayer coverage. With increasing Al deposition, they proposed that a mixed monolayer composed of the intermetallic phase plus Al metal is formed, followed by layer-by-layer growth of subsequent Al overlayers. When the coverage was increased from 0 to 3 ML, no new features were observed in the LEED pattern apart from a large increase of the background intensity, leading eventually to the disappearance of the substrate spots. The results appeared to be independent of the substrate faces either (111) or (110). Thus interface alloying could be expected to occur also for Al on Ag(100), even though this system has not yet been investigated.

In the following, we describe our results on the growth mode of Ag on Al(111) for coverages up to 5 ML as observed by the local probe of STM. We will resolve most of the puzzling and contradictory issues raised by the previous work. We will show that Shockley partial dislocations are formed that could account for the observations by Kim *et al.* described above. We will see that the film morphology, either rough or smooth, is strongly connected with the step morphology, either straight or meandering. We will also describe similar phenomena that we have observed during the first step of the growth of Al on Ag(100) for coverages up to 1 ML.

EXPERIMENTAL

The experiments were performed in two different ultra-high vacuum (UHV) chambers equipped with Omicron variable temperature STM apparatus. The crystals were polished down to 0.25 μm with diamond paste and cleaned in UHV by cycles of sputtering (Ar⁺, 1 kV, $T=573$ K) and annealing at 750 to 800 K for 1 to 2 h. Both evaporation of the pure elements to produce Al or Ag thin films, and STM measurements, were performed with the substrate at room temperature. The Ag source is an Omicron EFM3 electron-beam evaporator. The Al evaporator is an home-built vapor deposition source. The deposition fluxes were calibrated by determining the coverages from STM images in homoepitaxy experiments. The pressure during deposition was kept below 2×10^{-10} Torr.

RESULTS AND DISCUSSION

A. Ag on Al(111)

Figure 1 shows STM images of the Al(111) surface before and after exposure to 0.2 ML of Ag. The clean surface exhibits large terraces [Fig. 1(a)] upon which atomic-scale resolution is possible [inset to Fig. 1(a)]. The clean surface

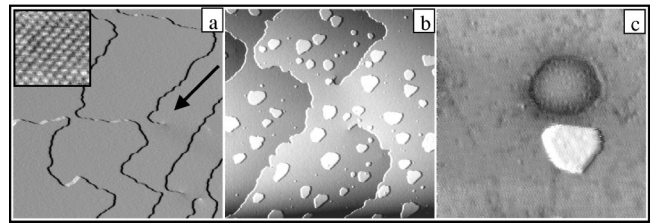


FIG. 1. (a) STM images ($200 \times 200 \text{ nm}^2$) of the clean Al(111) surface. The arrow points the screw dislocation. Inset: $2.5 \times 2.5 \text{ nm}^2$ image showing the hexagonal lattice. (b) Surface covered by 0.2 ML of Ag ($300 \times 300 \text{ nm}^2$). (c) STM image ($34 \times 34 \text{ nm}^2$) showing a dark hexagonal shape corresponding to a subsurface argon bubble. The bright triangles corresponds to an Ag island.

also exhibits some isolated defects including screw dislocations [arrow in Fig. 1(a)] and isolated subsurface argon bubbles with hexagonal shapes [Fig. 1(c)]. Subsurface noble gas bubbles in Al have already been identified and described by Schmid *et al.*^{10,11}

The effects of Ag deposition are illustrated in Fig. 1(b). Most of the Ag islands are roughly triangular in shape, and are 0.22 nm in height. In Ag/Ag(111) homoepitaxy, the islands usually adopt a more hexagonal shape.^{12,13} The triangular shape is due to the existence of two types of steps on a (111) surface, the so-called *A* and *B* steps, with (111) and (100) microfacets respectively. One type of step must be preferred energetically which leads to the observed approximately triangular shapes of the islands for Ag/Al(111). This island shape is nevertheless consistent with pseudomorphic growth of the Ag film.

Figure 2 shows STM images of the surface covered by 0.5 [Fig. 2(a)] and 1 ML of Ag [Figs. 2(b)–2(e)]. A pattern of double bright lines can be seen both on the substrate level and on the first and second layer levels. Their height is about 0.07 nm above the surface plane and the distance between two parallel lines is about 1.7 nm. They usually start and end at step edges of a terrace or an island [Figs. 2(b) and 2(c)]. They are arranged in a pattern with threefold symmetry [Fig.

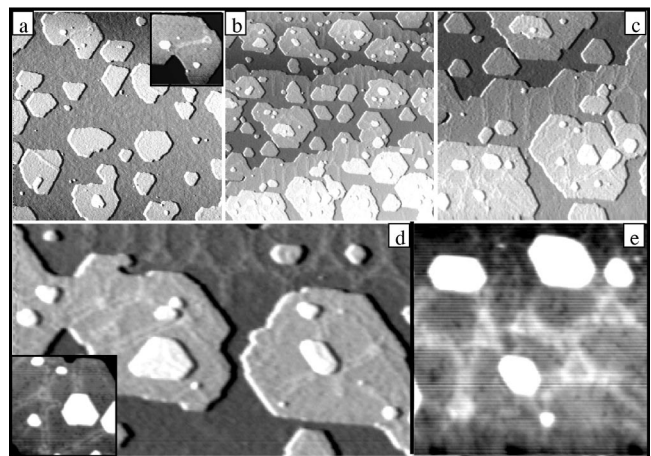


FIG. 2. STM images of the Al(111) surface covered by 0.5 ML (a) and 1 ML (b)–(e). (a) $200 \times 200 \text{ nm}^2$. Inset: $43 \times 43 \text{ nm}^2$, (b) $200 \times 200 \text{ nm}^2$, (c) $100 \times 100 \text{ nm}^2$, (d) $140 \times 50 \text{ nm}^2$, (e) $34 \times 34 \text{ nm}^2$.

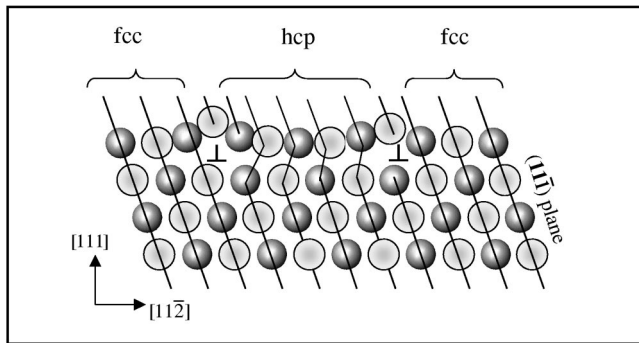


FIG. 3. (a) Schematic illustration of the atomic structure at partial dislocations between fcc and hcp stacking regions. The “ \perp ” symbols indicates the cores of the Shockley partial dislocations. Darker atoms are in the image plane and light gray atoms are $\frac{1}{4}[\bar{1}10]$ behind.

2(d) and inset]. When they connect together, they form small triangles with bright contrast [Fig. 2(e)].

This type of double-line arrangement has been observed by STM in many thin films deposited on close-packed surfaces.^{14–20} It results from the formation of misfit dislocations induced by the incorporation of adsorbed atoms in the top surface layer, therefore increasing the surface atom density.^{20,21} This is a basic mechanism for strain relief, which allows the density of the film to differ from that of the substrate. The basic structural ingredient is a stacking fault. It occurs on close-packed surfaces because, here, two types of high-coordination sites (fcc sites and hcp sites) are available for adsorption, with only a small difference in binding energy. For perfect pseudomorphic growth on the fcc substrate, only the fcc sites should be occupied. The formation of stacking fault domains, where atoms adopt the hcp sites, is a response of the system to the strain that builds up as the result of lattice mismatch. Indeed, the surface atomic density is necessarily changed in the narrow boundary regions between hcp and fcc domains, therefore partially relieving strain. These linear defects are characterized by a vector that shifts the atom positions from fcc stacking to hcp stacking (Burgers vectors of the type $\frac{1}{6}[2\bar{1}\bar{1}]$). Because the Burger vector is not a full lattice vector, the defects are called partial dislocations and are of the Shockley type in this case. In the narrow boundary regions between adjacent domains of fcc and hcp stacking, atoms must occupy intermediate sites between the two high symmetry hollow sites so they appear raised relative to the latter. This is the origin of the bright lines in the STM images. A schematic illustration of the atomic structure at partial dislocations between fcc and hcp stacking regions is provided in Fig. 3. Therefore, the double lines seen in the STM images of Fig. 2 are Shockley partial dislocations bounding hcp stacking fault domains. It might seem surprising that such a small lattice misfit between Ag and Al (less than 1%) induces the formation of such a dislocation network. However, even a system with zero lattice mismatch can exhibit such a structure. The herringbone reconstruction of clean Au(111) is made of the exact same partial dislocations.²² This is because atoms at the surface

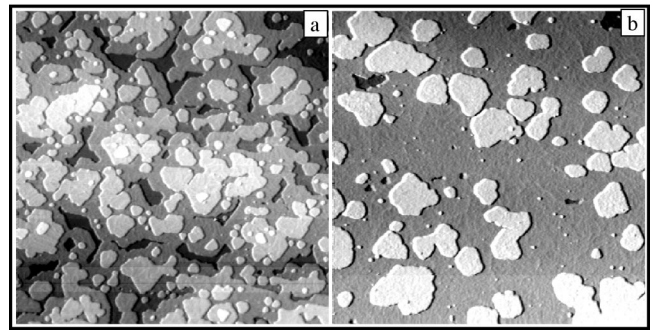


FIG. 4. STM images ($200 \times 200 \text{ nm}^2$) of the Al(111) surface covered by 2 ML (a) and 5 ML (b).

have a lower coordination number than bulk atoms and the associated strain is partially relieved by the reconstruction.

A second observation is that the step edges of both islands and terraces become straight with less kinks and corners, especially at 1 ML coverage. This is obvious if one compares the step edges of the STM images in Fig. 2 to those in Fig. 1. The straight steps are always perpendicular to the double lines, and hence the steps are parallel to the direction of strain relief. We note also that a significant amount of deposited element forms small islands on top of the first generation of islands. Therefore the film does not appear to grow in a layer-by-layer fashion in this coverage regime. The last two observations, step straightening and 3D growth, could be related to each other. Indeed, the importance of kink and corner sites in interlayer diffusion has been observed in several systems including Pt/Pt(111) and Co/Pt(111).²³ Straight steps, i.e., low density of kink and corner sites, could therefore inhibit interlayer mass transport leading to 3D growth.

As coverage increases further, the growth mode changes. Figure 4 shows two STM images of the same size ($200 \times 200 \text{ nm}^2$) covered by 2 and 5 ML of Ag, respectively. Here the deposition flux has been increased from 10^{-3} to 10^{-2} ML/s as compared to lower coverage experiments. At 2 ML [Fig. 4(a)], four different layers contribute significantly to the image, denoting a rather rough film. The steps are still straight, although this is less obvious than at 1 ML coverage. At 5 ML [Fig. 4(b)], the images reveal a very smooth film indicating that the growth mode has switched to layer-by-layer. At the same time, the steps have become very rough. Rough steps indicate a high density of kink and corner sites that could open channels for interlayer diffusion, consistent with the observed smooth growth. At this coverage, the Shockley partial dislocations are hardly seen: only a faint marbled appearance can be observed in the STM images. For this film thickness, the strain should now be at least partially released.

In Fig. 5, we show several STM images, taken at different times, of a single area on the surface after dosing with 0.05 ML of Ag. This observation was done in a preliminary experiment while the Al substrate may not have been sufficiently cleaned, as revealed by the presence of dark features inserted in the terraces [Fig. 5(c)] that could correspond to impurity oxygen atoms.^{10,24} Several straight bright lines are observed in these images. They are labeled *l1*, *l2*, and *l3*. The corrugation associated with these lines is about 0.09 nm

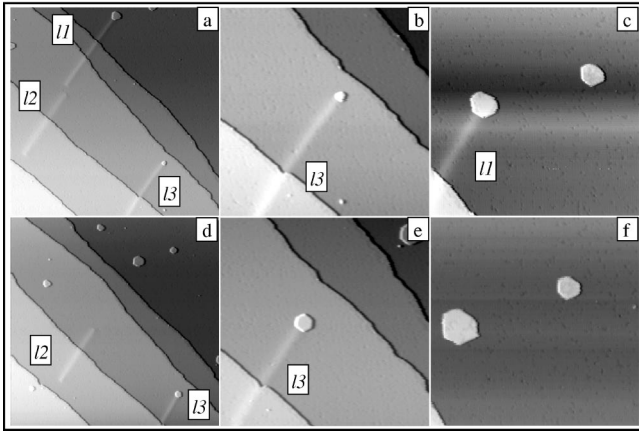


FIG. 5. STM images of the Al(111) surface covered by 0.05 ML of Ag. (a), (d) $225 \times 225 \text{ nm}^2$, (b), (e) $100 \times 100 \text{ nm}^2$, (c), (f) $80 \times 80 \text{ nm}^2$. Images of the top row were recorded before the images of the bottom row.

above the terrace level, similar to the Shockley partials described above. The lines can cross step edges. The lines $I1$ and $I3$ end at a Ag island. Comparing images 5(a) and 5(d), we see that $I1$ has disappeared during the several minutes that elapsed between acquisition of these two images. The images in Figs. 5(c) and 5(f) offer a closer view of the island ending $I1$. It is obvious that this island has become larger during the same time that $I1$ has disappeared. Its calculated surface increased from about 80 nm^2 at the beginning of the experiment [Fig. 5(c)] up to 140 nm^2 once $I1$ has disappeared [Fig. 5(f)]. The surface of the island that terminates line $I3$ also increases with time from 20 nm^2 [Fig. 5(b)] to about 60 nm^2 [Fig. 5(e)]. The line $I2$, which is not connected to any island, does not change on the timescale of the experiment. Lundgren *et al.* reported a similar phenomena resulting from growth of Co on Pt(111).²⁵ With atomically resolved STM images and chemical contrast, they could demonstrate that Co is incorporated in the topmost Pt layer creating misfit dislocations that dissociate into stacking fault regions bounded by partial Shockley dislocations appearing as double bright lines in the STM images, similar to what we reported in Fig. 2. For Co/Pt(111), the model suggests that Pt islands grow at the end of the double line reconstruction because this defect site allows easy exchange processes between Co adatoms and Pt surface atoms. There are, however, several differences between their observations and ours. First, in this experiment, we could not resolve the double line, which may be due to a poor tip condition or to rapid movement of atoms within these lines. Second, the double line reconstruction does not disappear as the island grows on Co/Pt(111), but instead is relatively mobile on the surface. In our case, it seems that the additional row of atoms in between the double lines is the reservoir from which the island grows. Atoms could be ejected from the top surface layer and diffuse in between the two Shockley partials toward the island. Images with higher resolution would be required to verify this scenario.

We now discuss our STM data in light of the previous observations on this system made with various experimental

techniques. First, recall that the disappearance of the LEED pattern reported by Kim *et al.*⁶ between 2 and 4 ML was interpreted as a consequence of interface alloy formation, most likely the hexagonal $\delta\text{-Ag}_2\text{Al}$ phase. Support for this interpretation came from the measured binding energy shift of the Ag $3d_{5/2}$ core level line by XPS.

Alloy formation is somewhat implausible, given what is known about the bulk phases. The Al-Ag phase diagram is well known and bulk alloy compounds are found over the whole range of composition. But these compounds are formed at elevated temperature, far above the room temperature at which Ag deposition occurs in our experiments. This does not rule out alloying however, since surface alloying has been observed in several systems induced by the interface strain (see Ref. 21 for a review). We already mentioned that Ag and Al have almost no miscibility at room temperature, but again it has been observed that elements immiscible in the bulk can sometimes intermix at the surface.²⁷

From the present STM analysis of Ag on Al(111), it is obvious that the disappearance of the LEED pattern reported by Kim *et al.*⁶ between 2 and 4 ML is related to the observed formation of stacking fault regions bounded by Shockley partial dislocations. At 2 ML, the density of the dislocations is high, and thus the density of stacking fault domains is also high. The disorder at the boundaries between the stacking fault domains should result in a large amount of incoherently scattered electrons therefore producing a large background in the LEED pattern. This is likely the reason for the disappearance of the LEED pattern reported by Kim *et al.* We therefore confirm that the adsorbate and substrate elements intermix at the interface, and this occurs *via* incorporation of adatoms in the surface layer and formation of the dislocation network. However, it seems more appropriate to describe this interface alloying in terms of a disordered solid solution rather than as an ordered hexagonal $\delta\text{-Ag}_2\text{Al}$ alloy. If such an ordered δ phase could be formed, then its signature should be observed in the LEED pattern. This interpretation is also consistent with the XPS data, since intermixing at the Shockley partial dislocations can account for the XPS binding energy shifts. Core level shifts are always observed when noble metals or late transition metals such as Pd are mixed with free electron metals such as Al, and these shifts are associated with a d -band filling.²⁶ Interestingly, metastable supersaturated Al-Ag dilute alloys are known to form Ag-rich precipitates in an Al matrix upon annealing the homogeneous solid solution at relatively low temperatures. The Ag atoms diffuse and form either spherical or plate-shaped precipitates. The precipitates are known as Guinier-Preston (GP) zones and γ plates, respectively. The plate-shaped precipitates are named for their atomic structure, which corresponds to the γ -hexagonal phase as identified by TEM. The orientation relationship with the Al matrix is $[0001]_{\text{hcp}} \parallel [111]_{\text{fcc}}$.²⁸ The formation of these flat precipitates corresponds to a planar transformation $\text{fcc} \rightarrow \text{hcp}$ which allows partial relief of the strain induced by the difference in atomic radii between the Ag solute and the Al matrix. Similarly, it is possible that annealing the film at relatively low temperature would induce the formation of the hexagonal Ag_2Al phase.

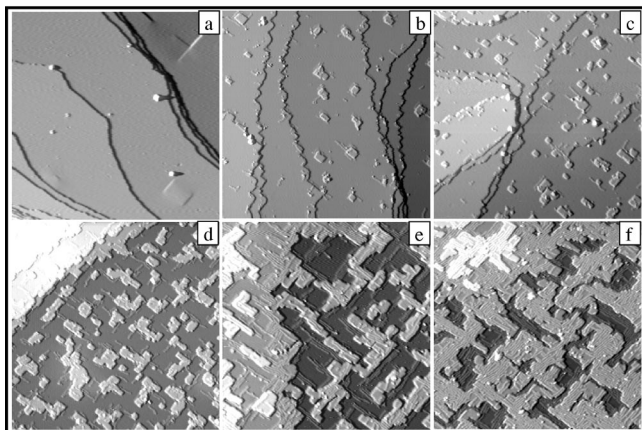


FIG. 6. STM images ($150 \times 150 \text{ nm}^2$) of the clean Ag(100) surface (a) and after exposure to 0.05 (b), 0.1 (c), 0.2 (d), 0.4 (e), and 0.8 ML (f) of Al.

For Ag films thicker than 5 ML, Kim *et al.* interpreted the reappearance of a sharp (1×1) LEED pattern as evidence for the existence of large Ag terraces, suggesting layer-by-layer growth. It was proposed that the large density of kink sites originating from the boundaries of stacking faulted islands could offer channels with reduced step edge barrier to promote interlayer diffusion. From our STM data in the same coverage regime, we confirm that the Ag film becomes surprisingly smooth. This is associated with step roughening and almost complete disappearance of the dislocations. However, the smoothing mechanism is different from what was proposed in Ref. 6. At this coverage, it seems that the stacking fault domains are buried, as the double lines are not seen anymore. The film should now be made of only fcc stacking very similar to a Ag(111) surface. But differences must exist to explain why the Ag film grows 2D instead of 3D as in Ag/Ag(111) homoepitaxy. One difference with homoepitaxy may be the roughness of the steps, which provides a high density of kink and corner sites. The step edge barrier for an adatom to diffuse downward associated with these sites could well be considerably lower than for straight *A* and *B* type steps and thus could provide an explanation for the different growth mode observed. The origin of the step roughness is unclear. We exclude the possibility that residual gas in the resting chamber or generated by the evaporator itself might be the cause of step roughening. If this had been the case, then step roughening would have also occurred at lower coverage. Instead, step straightening is observed at 1 and 2 ML coverage. The step roughening must be related to strain in the film. Indeed, if the film were fully relaxed, the situation should be exactly equivalent to Ag/Ag(111) homoepitaxy with 3D growth mode. The observation that the terraces have still a faint marbled aspect is certainly an indication that the interfacial strain is not yet totally accommodated.

B. Al on Ag(100)

We now present the results of a related study of the growth of Al thin films on the Ag(100) surface. Here, the

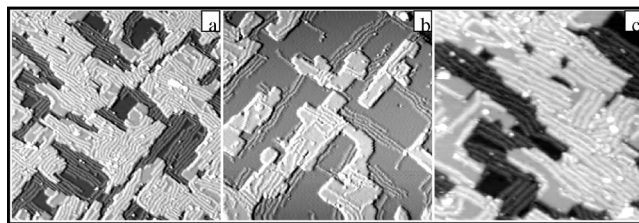


FIG. 7. STM images of the Al film deposited on Ag(100). (a) $100 \times 100 \text{ nm}^2$, 0.8 ML, (b) $80 \times 80 \text{ nm}^2$, 0.4 ML, (c) $100 \times 100 \text{ nm}^2$, 0.4 ML.

maximum coverage was limited to 1 ML. Figure 6 shows a sequence of STM images of the Ag(100) surface covered by 0.05 up to 1 ML of Al. Starting from 0.05 ML, bright stripes appear in addition to the square-shaped Al islands. The stripes are 0.07 nm above the terrace plane and their average width is 1.2 nm. They are best viewed in Fig. 7. The density of these stripes increases very quickly with coverage, forming a dense network at 1 ML, with a symmetry reflecting the fourfold symmetry of the surface. At the same time, a very sharp faceting of the step is observed. For coverage as low as 0.05 ML, the steps are made of straight segments oriented most likely along the dense $[01\bar{1}]$ and $[011]$ directions, leaving very few kink sites. The step orientations are the same as for stripes. In this case, we could also perform a LEED experiment. At 1 ML, the sharp LEED spots of the clean substrate have almost completely disappeared in an intense background.

The strain relief provided by close-packed stacking faults has been studied mainly for hexagonal substrates but it exists also for substrates with square symmetry. Müller *et al.* reported the appearance of linear stripes during the growth of Cu on Ni(100).²⁹ The proposed model involved again stacking fault regions in (111) planes, therefore inclined with respect to the (100) surface. The bright lines observed in our STM images could result from a similar type of surface reconstruction induced by lattice misfit accommodation or simply surface strain relief. In this model, the width of the stripes is expected to increase with coverage. We note also that the density of the dislocation lines appears to be too high considering the very small lattice mismatch between Al and Ag. Another hypothesis is that the stripes revealed by STM result from a surface reconstruction induced by a surface alloying. Additional work is needed to clarify this point. Nevertheless, both interpretations are consistent with a strong intermixing of Al and Ag atoms at the interface.

CONCLUSION

Our results demonstrate the influence of interfacial strain on the growth modes of Ag films on Al(111), despite the small magnitude of the lattice misfit in this system. The strain is relieved by the formation of stacking fault domains bounded by Shockley partial dislocations that appear as double bright lines in the STM images. Intermixing of the elements at the substrate-film interface results at the dislocations. Interface alloying therefore occurs but rather in the form of a disordered solid solution than an extended ordered

alloy. The growth mode and the step shape appear to be strongly connected. The growth is 3D as long as the steps are straight but switches to 2D at higher coverage when the steps become rough. This occurs at about 5 ML, where the dislocation network disappears and the film is nearly fully relaxed. Most likely, step straightening is related to the anisotropic strain relaxation which occurs only in directions perpendicular to the double lines, i.e., along *A* and *B* step directions. We also reported related observations made on Al deposited on the Ag(100) square substrate. A dense network of bright stripes with fourfold symmetry is observed in the STM images, together with step straightening, and the LEED pattern disappears at 1 ML. The bright lines result from a surface reconstruction induced either by lattice misfit accom-

modation, involving “inclined” stacking fault regions in (111) planes or surface alloying.

ACKNOWLEDGMENTS

This work was supported by NSF Grant No. CHE-0078596, and performed at Ames Laboratory (which is operated for the U.S. DOE by ISU under Contract No. W-7405-Eng-82). One of us (J.L.) acknowledge funding from EPSRC Grant No. GR/N18680. We wish to thank A. K. Schmid for an enlightening introduction to Shockley partial dislocations and critical reading of the manuscript, and A.-P. Tsai for interesting suggestions about this work.

*Present address: LSG2M, CNRS-UMR 7584, Ecole des Mines, F-54042 Nancy, France.

†Email address: Vincent.Fournee@mines.u-nancy.fr

‡Present address: Brookhaven National Laboratory, P.O. Box 5000, Upton, NY 11973-5000.

¹E. Bauer, *Z. Kristallogr.* **110**, 372 (1958).

²E. Bauer and J. H. van der Merwe, *Phys. Rev. B* **33**, 3657 (1986).

³H. Brune, *Surf. Sci. Rep.* **31**, 121 (1998).

⁴L. Vitos *et al.*, *Surf. Sci.* **411**, 186 (1998).

⁵A. Losch and H. Niehus, *Surf. Sci.* **446**, 153 (2000).

⁶S. H. Kim *et al.*, *Phys. Rev. B* **63**, 085414 (2001).

⁷J. Vrijmoeth *et al.*, *Phys. Rev. Lett.* **72**, 3843 (1994).

⁸K. Bromann *et al.*, *Phys. Rev. Lett.* **75**, 677 (1995).

⁹W. J. Wytenburg, R. M. Ormerod, and R. M. Lambert, *Surf. Sci.* **282**, 205 (1993).

¹⁰M. Schmid *et al.*, *Phys. Rev. Lett.* **76**, 2298 (1996).

¹¹M. Schmid, S. Crampin, and P. Varga, *J. Electron Spectrosc. Relat. Phenom.* **109**, 71 (2000).

¹²K. Morgenstern, G. Rosenfeld, and G. Comsa, *Surf. Sci.* **441**, 289 (1999).

¹³M. Giesen, *Prog. Surf. Sci.* **68**, 1 (2001).

¹⁴J. V. Barth *et al.*, *Phys. Rev. B* **42**, 9307 (1990).

¹⁵H. Brune *et al.*, *Phys. Rev. B* **49**, 2997 (1994).

¹⁶C. Günther *et al.*, *Phys. Rev. Lett.* **74**, 754 (1995).

¹⁷M. Hohage, T. Michely, and G. Comsa, *Surf. Sci.* **337**, 249 (1995).

¹⁸A. K. Schmid *et al.*, *Phys. Rev. Lett.* **78**, 3507 (1997).

¹⁹B. Fischer *et al.*, *Phys. Rev. Lett.* **82**, 1732 (1999).

²⁰J. de la Figuera *et al.*, *Phys. Rev. B* **63**, 165431 (2001).

²¹R. Q. Hwang and M. C. Bartelt, *Chem. Rev.* **97**, 1063 (1997).

²²C. B. Carter and R. Q. Hwang, *Phys. Rev. B* **51**, 4730 (1995).

²³M. Schmid *et al.*, *Appl. Phys. A: Mater. Sci. Process.* **72**, 405 (2001).

²⁴H. Brune *et al.*, *Phys. Rev. Lett.* **68**, 624 (1992).

²⁵E. Lundgren *et al.*, *Surf. Sci.* **423**, 357 (1999).

²⁶J. C. Fuggle *et al.*, *Phys. Rev. B* **16**, 750 (1977).

²⁷H. Röder *et al.*, *Phys. Rev. Lett.* **71**, 2086 (1993).

²⁸K. T. Moore and J. M. Howe, *Acta Mater.* **48**, 4083 (2000).

²⁹B. Müller *et al.*, *Phys. Rev. Lett.* **76**, 2358 (1996).